NOISE SOURCE IDENTIFICATION ON A CONTINUOUS MINING MACHINE

Hugo E. Camargo, Adam K. Smith, Peter G. Kovalchik, Rudy J. Matetic
National Institute for Occupational Safety and Health – PRL
626 Cochrans Mill Road, Pittsburgh, PA 15236

ABSTRACT

Noise Induced Hearing Loss is the most common occupational disease in the U.S. and of paramount importance in the mining industry. According to data for 2006 from the Mine Safety and Health Administration (MSHA), Continuous Miner operators accounted for 30.2% of underground mining equipment operators with noise doses exceeding the Permissible Exposure Limit (PEL). This figure becomes more significant considering that 49% of the 2006 national underground coal production was extracted using continuous mining methods. Thus, there is a clear need to reduce the sound radiated by Continuous Mining Machines. The first step towards efficient noise control of a Continuous Mining Machine requires identification of the various noise sources under controlled operating conditions. To this end, a 42-microphone phased array was used in conjunction with 4 reference microphones to sample the acoustic field of a machine in the Hemi-anechoic chamber of the Pittsburgh Research Laboratory. These data were processed using a frequency-domain beamforming algorithm to obtain acoustic maps of 5 sides of the machine. The focus of the test was on the conveyor noise since previous studies showed that operation of the conveyor is the most important contributor to the sound radiated by the machine. From the acoustic maps, the following potential areas for noise control were identified, and included: chain-tail-roller interaction, chain flight tip-side board interaction, and chain-upper deck interaction.

INTRODUCTION

In today's industrialized world, noise constitutes one of the most common environmental and occupational hazards. Consequently, occupational Noise Induced Hearing Loss (NIHL) has been recognized by the National Occupational Research Agenda (NORA) as the most common job related diseases in the U.S[1]. Particularly in the mining industry, noise has been found to have the most devastating consequences. According to a study conducted by the National Institute for Occupational Safety and Health (NIOSH), 90% of coal miners and 50% of metal/non-metal miners had hearing loss by age 50, in contrast to 10% of those who were not exposed to occupational noise[2].

One of the most common extraction methods in the mining industry is the continuous mining. In this method, a self propelled machine known as the Continuous Miner (CM), controlled by an operator and its helper, rips coal from the face and loads it into conveyors or shuttle cars in a continuous operation. In 2006, 49% of the total coal production in the U.S. was extracted using this method[3].

Analysis of noise samples collected by the Mine Safety and Health Administration (MSHA) in 2006 revealed that of the various mining equipment operators, 30.2% of CM operators were exposed to noise levels exceeding the Permissible Exposure Level (PEL) stipulated in the Title 30 of the Code of Federal Regulations[4] (see Appendix A). This constitutes the largest group of overexposed mining equipment operators that according to the Bureau of Labor Statistics employs approximately 9660 people[5]. Other mining equipment with overexposed operators were Roof Bolters (20.1%), Bulldozers (10.0%), Shuttle Cars (3.6%), and Longwall Shearers (2.6%).

In this context, NOISH is currently conducting research aimed at reducing the noise radiated by the CM. Efficient noise control of a CM requires Noise Source Identification (NSI). This process involves the determination of the spatial location, as well as the frequency content of the dominant sources. Traditionally, NSI has been performed by conducting acoustic intensity measurements over a grid enclosing the device under test. However, this approach is very time intensive as it requires

the acquisition of data at every grid point for a single test configuration.

The use of phased array technology for noise source identification is a relatively new technique that is very time efficient. This technique consists of collecting acoustic pressure data using an array of microphones and processing the data with a beamforming algorithm.

The present work describes the use of phased array technology for noise source identification on a CM. The three main components that radiate noise from a CM are the cutting head, the conveyor and the dust collector fan, which are shown in Figure 1. Of these three components it was determined that conveyor is the most significant contributor to the total radiated sound[6].

Figure 1. Noise generating components on a CM.

Previous studies involved measurements of Sound Pressure Level (SPL) over a grid enclosing the entire machine on a quasi free field environment[6]. Results from these measurements showed that most of the sound was being generated at the tail section of the CM. However, it was not clear what mechanisms or sources were generating these high noise levels in this area of the CM. Consequently, conveyor noise has been the subject of previous research[6,7,8]. From these studies, three noise controls were proposed: 1) A jacketed Tail Roller (TR), i.e. a resilient material between an inner and an outer steel shell, 2) a urethane-coated Tail Roller, and 3) urethane-coated chain flights. Figure 2 shows these noise controls.

(a) (b) (c)

Figure 2. Controls for tail section noise: a) Jacketed TR, b) urethane-coated TR, and c) urethane-coated chain flights.

Use of a urethane-coated TR resulted in a noise reduction of 2 dB(A) in Sound Power Level. However, the main drawback of this control was its durability when tested underground it only lasted 10 days of operation before the urethane was torn from the roller. A standard TR is not replaced until the CM is rebuilt. The jacketed TR yielded a modest reduction of approximately 1 dB(A) in Sound Power Level. The most promising control was the chain with urethane-coated flights. Implementation of this control attenuated the Sound Power Level by 10 dB(A)[6].

NOMENCLATURE

$y_n(t)$	Acoustic pressure recorded by microphone n.
$Y(f)$	Fourier Transform of $y(t)$.
$p(x_b,t)$	Acoustic pressure induced by a source at x_b.
$P(f)$	Fourier Transform of $p(t)$.
g	Free-field Green's function.
Δt	Propagation time between source and observer.
$b(x_b)$	Beamform output.
R	Resolution in terms of the spotsize [m].
λ	Acoustic wavelength [m].
L	Distance between array and potential source [m].
D	Diameter of the array [m].
psf	Point Spread Function.

EXPERIMENTAL SETUP

Acoustic measurements were conducted in the Hemi-Anechoic chamber of Pittsburgh Research Laboratory (PRL). This is a 17.7-meter long by 10.4-meter wide by 7.0-meter high chamber that meets the requirements of ISO 3744 down to approximately 100 Hz. The device under test was a new JOY 14CM-15 Continuous Miner provided with a 38-inch wide 54-flight conveyor chain. The chain was set under tension by means of a hydraulically controlled take up system. Figure 3 shows the CM in the Hemi-Anechoic chamber.

Figure 3. Continuous Miner in the Hemi-Anechoic chamber.

Data were collected using a 1.92-meter 42-element Bruel & Kjaer microphone phased array. The array has a spoke-wheel configuration with a total of seven arms, each holding 6 microphones. Due to the large size of the CM with respect to the array, various measurements along the sides, front, back, and overhead of the CM were performed. Figure 4 shows the various positions of the array with respect to the CM at which data was collected. For the side, front and back measurements, the array was at a distance of 2 meters from the CM, whereas for the overhead measurements the array was at 1.75 meters. In addition to the phased array measurements, the Sound Power radiated by the CM was measured in PRL's reverberation chamber[9], according to the ISO3743-2 standard.

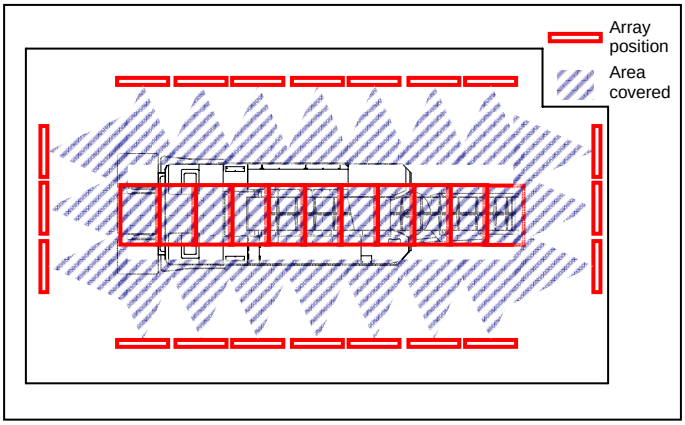

Figure 4. Phased array positions with respect to the CM in the Hemi-Anechoic chamber.

During normal operation of the conveyor, i.e. moving coal from the front to the back of the CM, coal has a damping effect on the noise radiated by the conveyor. Previous work at PRL showed that a continuous water flow supplied to the middle of the conveyor has the same effect as coal. Therefore, in order to simulate the noise damping effect of coal, a water flow rate of 4 gal/min was used in the present test.

BEAMFORMING

The underlying principle on which beamforming theory was developed is that a noise source is sensed by the microphones in the array with a time delay, i.e. phase shift, and amplitude differences as shown in Figure 5. It is these differences that are used to identify the location and the strength of the source. The array is electronically steered to each potential source point of interest by adjusting the phase of the microphone data. The approach to make this phase adjustment is to assume a noise source exists at each potential point of interest, x_b. The simplest and most commonly used source model is that of a monopole given by:

$$p(x,t) = \frac{s(t - r/c)}{4\pi r}, \qquad (1)$$

where p is the acoustic pressure perceived at time t by the observer located at x; s is the signal emitted by the monopole located at x_s, r is the distance between the source position and the observer position, and c is the speed on sound.

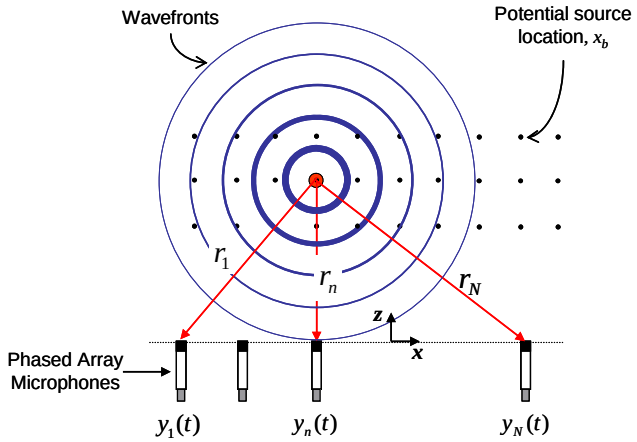

Figure 5. Phased array measurements of a point source.

The frequency-domain model of equation (1) is given by:

$$P(x, f) = S(f)g(x, f), \qquad (2)$$

where f is the frequency in Hz, $S(f)$ is the Fourier Transform of $s(t)$ and $g(x,f)$ is the free-field Green's function:

$$g(x, f) = \frac{e^{-i2\pi f\Delta t}}{4\pi r} \qquad (3)$$

Δt is the time required for the sound to travel from the source at x_b to an observer located at x, and thus it is also known as the propagation time:

$$\Delta t = r / c \qquad (4)$$

For an array of N-microphones, at each potential source point of interest x_b, the following expression is evaluated:

$$b(x_b) = \frac{\mathbf{g}^*(x_b)}{\|\mathbf{g}(x_b)\|}\mathbf{Y}(f)\mathbf{Y}^*(f)\frac{\mathbf{g}(x_b)}{\|\mathbf{g}(x_b)\|} \qquad (5)$$

where $\mathbf{Y}(f)$ is a vector containing the Fourier Transforms of the time series of the acoustic pressure recorded by each microphones of the array:

$$\mathbf{Y}(f) = \begin{bmatrix} Y_1(f) \\ Y_2(f) \\ \vdots \\ Y_N(f) \end{bmatrix}, \qquad (6)$$

and $\mathbf{g}(x_b)$ is a vector containing the acoustic pressure induced at the array microphones by the assumed source at x_b, given by the free-field Green's function:

$$\mathbf{g}(x_b) = \begin{bmatrix} g_1(f) \\ g_2(f) \\ \vdots \\ g_N(f) \end{bmatrix} \tag{7}$$

The normalized vectors $\boldsymbol{g}(x)/\|\boldsymbol{g}(x)\|$, are also known as the steering vectors and are usually denoted as $\boldsymbol{w}(x)$. The beamform expression $b(x_b)$ represents an estimate of the acoustic pressure-squared at the array location caused by the source at x_b.

The product $\mathbf{Y}(f)\mathbf{Y}^*(f)$ is the cross-spectral matrix of the microphone data. The diagonal elements of this matrix are the auto-powers which do not carry phase information but usually contain microphone self noise. Therefore, in order to improve the beamform output, these diagonal elements are usually removed from the cross-spectral matrix and are substituted by zeros. This process is also known as Diagonal Removal (DR).
In order to evaluate the performance of a microphone phased array at any frequency of interest, a simple point source is simulated at some desired distance from the array center. Then, using a beamforming algorithm, an acoustic map of this simulated source is computed. This particular acoustic map is also known as the array beam pattern or the array Point Spread Function (*psf*)[10], and is given by:

$$psf(x_b, x_S) = \left\| \mathbf{w}^*(x_b)\mathbf{w}(x_S) \right\|^2 \tag{8}$$

The Point Spread Function of a phased array contains a main-lobe and various side-lobes. The main-lobe is due to the simulated source. However, the side lobes are purely mathematical, i.e. do not represent any simulated source, and are a consequence of the finite number of microphones in the array. Therefore, the *psf* yields information regarding: 1) the resolution of the acoustic maps also known as the spotsize which is defined as the width of the main-lobe 3 dB down from its peak value, and 2) the dynamic range, that is the difference between the main-lobe peak value and the maximum side-lobe peak value. The variables that determine the resolution R of the acoustic maps are the size of the array D, the distance between the array and the source L, and the frequency of interest represented by the wavelength λ. The following expression can be used as a rule of thumb[11]:

$$R = 1.22\lambda L / D \tag{9}$$

Equation (9) was used to compute the resolution of the array at three different source-array distances used in the present test. Figure 6 shows these values as a function of frequency.

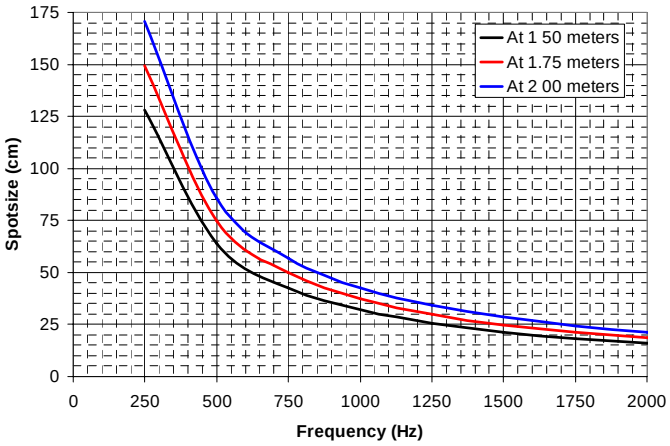

Figure 6. Resolution of the array used in the present test for source located at three different distances.

From Figure 6 it can be observed that for this particular array and test setup, a moderate resolution is obtained for frequencies between 400 Hz and 1000 Hz. However, for frequencies above 1000 Hz, the spotsize compared to the dimensions of the machine imparts a good resolution.

RESULTS

Phased array data were processed using a frequency-domain beamforming algorithm that removes the diagonal elements of the cross-spectral matrix. Beamform output was obtained in the form of 1/3-octave band acoustic maps. The frequency range of interest was 400 Hz to 3150 Hz. Sound power measurements in a reverberation chamber revealed that around 91% of the acoustic power radiated by a CM is emitted in this frequency range. Figure 7 shows the A-weighted sound power measured in a reverberation chamber.

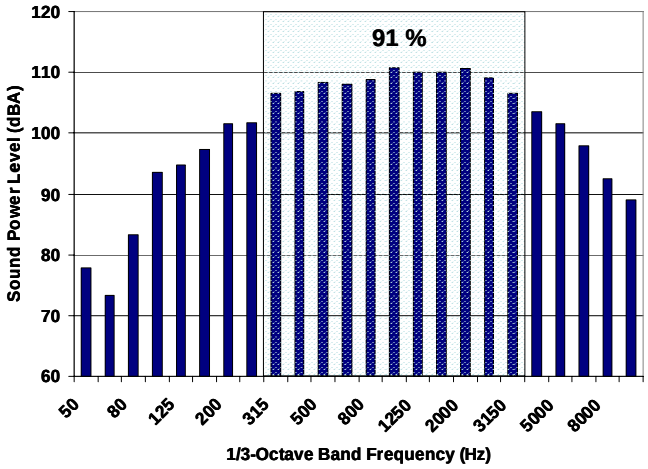

Figure 7. A-Weighted Sound Power Level emitted by the CM with the conveyor operating in a reverberation chamber.

Overhead measurements revealed dominant noise sources located at the tail section of the CM; more specifically in the vicinity of the tail roller. Examination of the acoustic maps suggests three different noise mechanisms: 1) Chain-tail roller interaction, 2) flight tip-side board interaction, and 3) flight-upper deck interaction. Figure 8 shows these sources at four different frequencies.

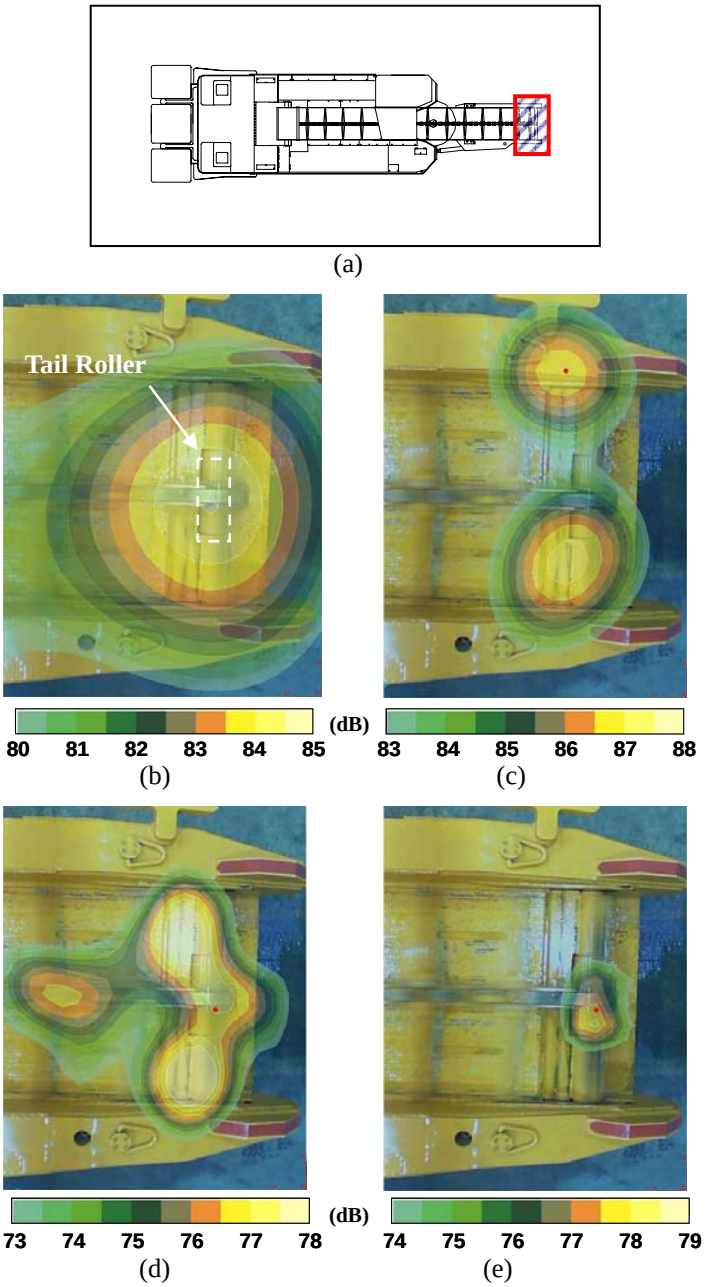

Figure 8. Dominant sources. a) Covered area by the acoustic maps at b) 500 Hz, c) 1000 Hz, d) 1600 Hz, and e) 2500 Hz.

The acoustic maps shown in Figure 8 unveil three different types of noise sources that were previously suspected but not confirmed. It can be seen that not only the impacts from the chain links onto the tail roller generate the noise at the tail section. The impacts from the flight tips onto the side boards, and the impacts from the chain flights onto the upper deck are also significant noise radiators; this explains why the coated flight chain, which attenuates these impacts, yielded the most promising results. Therefore, a combination of both the coated TR and the chain with urethane-coated flights is required to effectively reduce the strength of the sources at the tail section.

Secondary sources were identified at the front end of the left flex-board guide at 1600 Hz and 2000 Hz as shown in Figure 9. It is suspected that impacts from the chain flight tips cause the flex-boards to vibrate which in turn rattle against the guides. Since there is a small clearance of approximately 1 cm between the flexi-boards and the flight tips, a small transverse displacement of the chain will cause a shift of the impacts from the right to the left flex-boards and vice versa. A similar phenomenon was observed in previous studies when the vibration of the left flex-plate was larger than that of the right flex-plate[8].

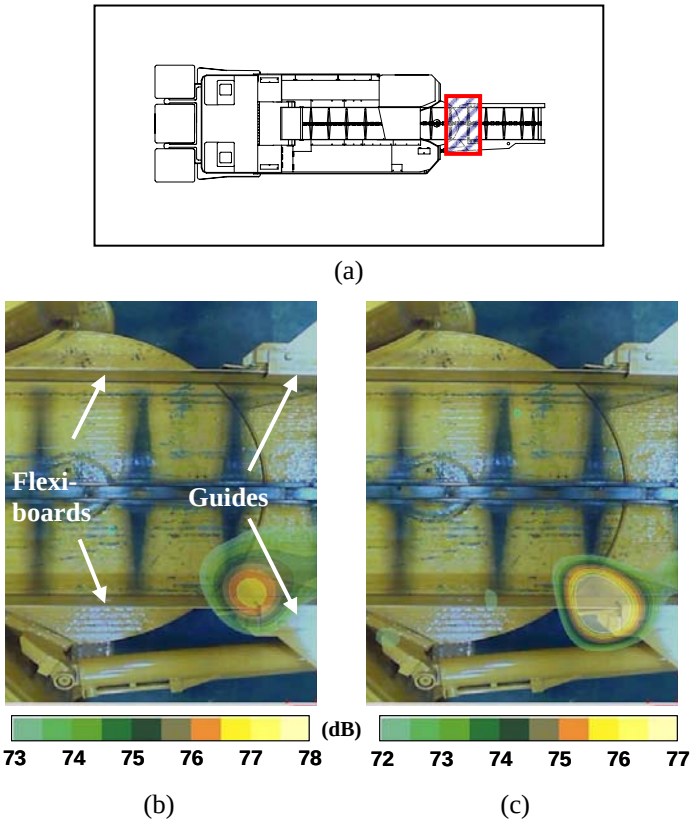

Figure 9. Secondary sources. a) Covered area by the acoustic maps at b) 1600 Hz, and c) 2000 Hz.

Measurements with the array at the rear of the CM confirmed the three noise mechanisms suggested by the overhead measurements. Figure 10 shows the acoustic maps obtained

with the array at the back for the same frequencies shown in Figure 8.

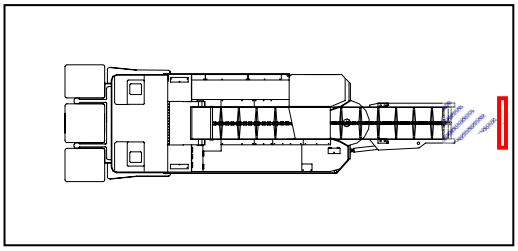

(a)

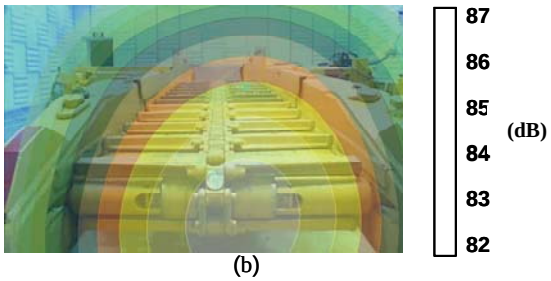

(b)

(c)

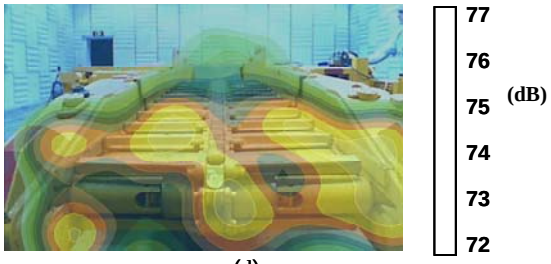

(d)

(e)

Figure 10. Dominant sources. a) Covered area by the acoustic maps at b) 500 Hz, c) 1000 Hz, d) 1600 Hz, and e) 2500 Hz.

Acoustic maps from the left side of the CM show two dominant sources: 1) at an opening of the lower deck where the tail section pivots right and left, and 2) at the place where the chain enters the lower deck upon leaving contact with the tail roller. Figure 11 shows these two noise source locations.

Acoustic maps from the right side of the CM reveal a source at the place where the flexi-board interacts with the guide, as shown in Figure 12 on pg 7. Note that overhead results in Figure 8 show a noise source at the left flexi-board-guide interaction place and none on the right side. However, it should be kept in mind that these measurements were taken at different times and thus the triggering mechanism, i.e. the impacts from the flight tips to the flexi-boards, probably shifted from left to right.

Measurements were also conducted with the array in front of the CM. Since the focus of this work was on conveyor noise, the cutting head of the CM was raised, leaving a direct view to the front part of the conveyor. Acoustic maps from these measurements show a dominant source where the chain engages the upper deck. Figure 13 shows this source at 1600 Hz and 2000 Hz. However, considering the operators location, shown in Figure 13a, these sources are not as significant as those in the tail section. Furthermore, use of a coated chain will also reduce the strength of this source.

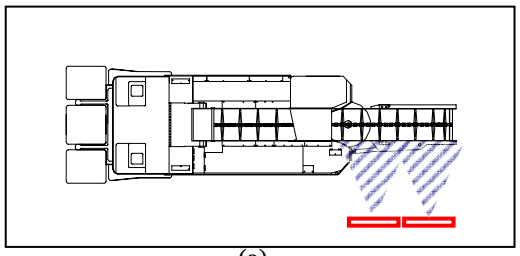

(a)

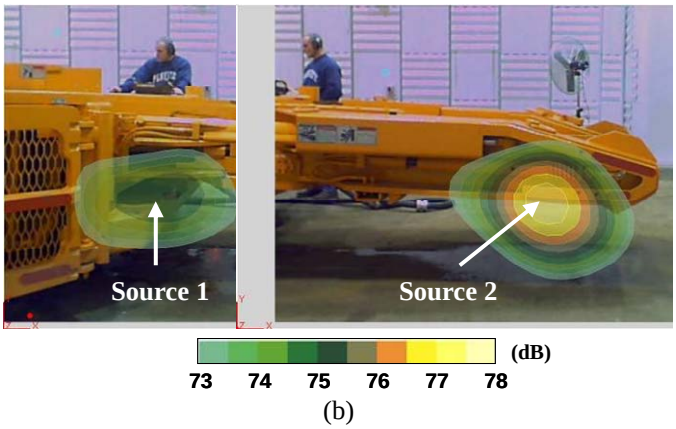

(b)

Figure 11. Sources on the left side of the CM. a) Covered area by the acoustic maps at b) 1250 Hz.

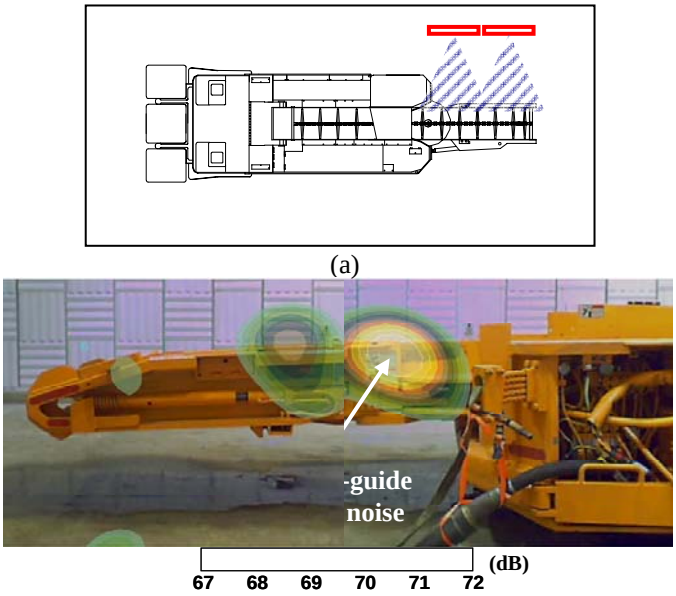

(a)

(b)

Figure 12. Sources on the right side of the CM. a) Covered area by the acoustic maps at b) 1600 Hz.

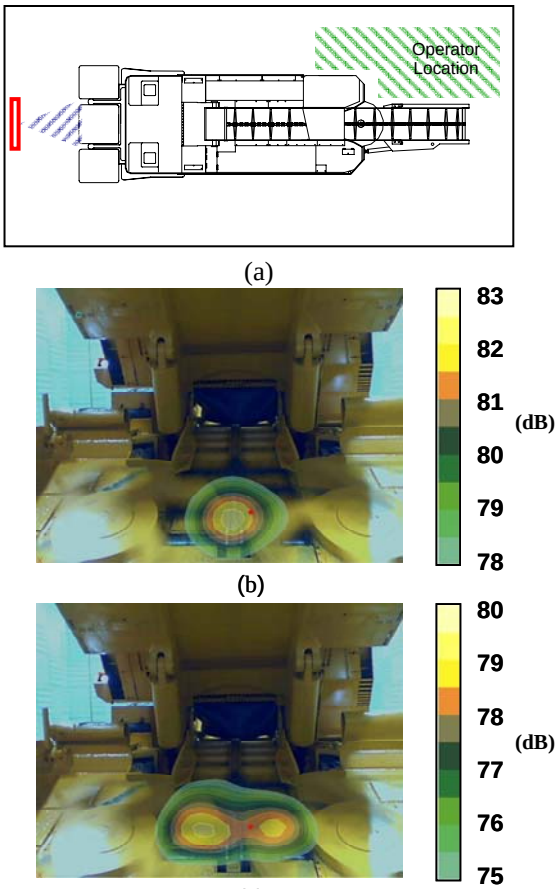

(a)

(b)

(c)

Figure 13. Sources on the front of the CM. a) Covered area by the acoustic maps at b) 1600 Hz, and c) 2000 Hz.

CONCLUSIONS

Noise source identification on a CM was performed using phased array measurements and a frequency domain beamforming algorithm with Diagonal Removal. The focus of this test was on conveyor noise. Dominant noise sources were identified at the tail section of the CM. Acoustic maps obtained with the array overhead and in the back of the CM reveal that not only the impacts from the chain onto the tail roller generate noise at the tail section, but also the impacts from the chain flights onto the side boards and onto the upper deck are significant noise radiators. Therefore, in order to effectively reduce the noise radiated by the tail section of the CM, a combination of both a coated tail roller and a chain with urethane-coated flights will be required. Even tough the coated TR exhibited durability issues, the advent of new engineering materials such as carbon fiber and Kevlar composites opens the possibility for further research on this control.

A noise source was identified at the front of the CM, in the place where the chain engages the upper deck. However, since this source is located away from the operator's position, it is not considered as significant as the noise sources at the tail section. Secondary noise sources were also identified at the guides of the flexi-boards. It is suspected that the impact from the flight tips onto the flexi-boards triggers these sources. Most of these noise sources can be attenuated by implementation of a chain with urethane-coated flights.

Based on these results, future work will involve testing tail rollers coated with urethane of different hardness. Also, the acoustic performance of flexi-boards with constrained layer damping will be investigated.

ACKNOWLEDGMENTS

The authors would like to thank JOY Mining Manufacturing Co. for providing the CM. Thanks are also due to Lynn Alcorn and Patrick McElhinney for their help and support during the test.

REFERENCES

[1] Smith, A.K., Spencer, E.R., and Alcorn, L.A., "Underground Evaluation of Coated Flight Bars for a Continuous Mining Machine", Proceedings of Inter-Noise 2006, Honolulu, Hawaii, USA, Dec. 3-6, 2006.

[2] Franks, J.R., "Analysis of Audiograms for a Large Cohort of Noise-Exposed Miners", National Institute for Occupational Safety and Health, Internal report, Cincinnati, OH,1996.

[3] Energy Administration Information website, Underground Coal Production by State and Mining Method, Data for 2006, http://www..eia.doe.gov/cneaf/coal/page/acr/table3 html.

[4] MSHA [2008]. MSHA Standardized Information System, Number of Noise Samples @90PELDose(computed)>=100 by Machine Code, 2006. Denver, CO: U.S. Department of Labor, Mine Safety and Health Administration, Office of Injury and Employment Information. Date accessed: March 20, 2008.

[5] Bureau of Labor Statistics website, Occupational Employment and Wages, May 2006, 47-5041 Continuous Mining Machine Operators, http://www.bls.gov/oes/current/oes475041.htm.

[6] Kovalchik, p., Johnson, M., Burdisso, R., Duda, F., and Durr. M., "Noise Control for Continuous Miners", Proceedings from the 10th International Meeting on Low Frequency Noise and Vibration and its Control, York, England, Sept. 11-13, 2002, PP. 299-306.

[7] Smith, A.K., Spencer, E.R., Alcorn, L.A., and Kovalchik, P.G., "Underground Evaluation of Coated Flight Bars for Continuous Mining Machines", Inter-Noise 2006 Proceedings, Dec. 3-6, 2006, Honolulu, Hawaii, USA.

[8] Smith, A.K., Yantek, D.S., and Peterson, J.S., "Development and Evaluation of a Urethane Jacketed Tail Roller for Continuous Mining Machines", Proceedings from IMECE2007, IMECE2007-41821, Seattle, Washington, Nov. 11-15, 2007.

[9] Peterson, J.S., and Bartholomae, R.C., "Design and Instrumentation of a Large Reverberation Chamber", Proceedings of Noise-Con 2003, Cleveland, Ohio, June 23-25, 2003.

[10] Muller, T.J. (Editor), *Aeroacoustic Measurements*, Springer, 2002.

[11] Christensen, J.J., and Hald, J., B&K, "Beamforming", Bruel & Kjaer Technical Report No 1-2004.

APPENDIX A

Permissible Exposure Level

According to the Title 30 Code of Federal Regulations, Section 62.101, the Permissible Exposure Level is a Time-Weighted Average for an 8-hour shift (TWA_8) of 90 dB(A). This value is equivalent to a dose of 100% of that permitted by the standard, given by:

$$D = 100\left(\frac{C_1}{T_1} + \frac{C_2}{T_2} + \cdots + \frac{C_n}{T_n}\right) \qquad \text{(A.1)}$$

where C_n is the time a miner is exposed to a specific sound level and T_n is the reference duration exposure for that specific sound level, given by the following expression:

$$T_n = \frac{8}{2^{(L_n - 90)/5}} \qquad \text{(A.2)}$$

where L_n is the measured A-weighted, slow-response sound pressure level.

Once the dose percentage D is computed using equations (A.1) and (A.2), the equivalent TWA_8 can be obtained from:

$$TWA_8 = 16.61 \cdot \log_{10}(D/100) + 90 \qquad \text{(A.3)}$$

Equation (A.3) yields the TWA_8 which represents the sound level that, if constant throughout the 8-hour shift, would result in the same measured dose D.